PROCEEDINGS OF SCIENCE

High-p_T experimental results on QCD at the LHC.

Javier Llorente, on behalf of the ATLAS and CMS Collaborations[a,*]

[a] *Simon Fraser University*

E-mail: javier.llorente.merino@cern.ch

Measurements by the ATLAS and CMS Collaborations, sensitive to various aspects of the modelling of QCD, are presented. This includes the production of jets, inclusively and in association with Z bosons, as well as the production of photon pairs and the fragmentation of heavy quarks into hadrons. The measurements are compared to fixed-order perturbative predictions where available, as well as to Monte Carlo simulations including different algorithms for the matrix element calculation, the parton shower emissions and the hadronisation model. Determinations of the parton distribution functions inside the proton are also presented by both Collaborations.

The Tenth Annual Conference on Large Hadron Collider Physics - LHCP2022
16-20 May 2022
online

*Speaker

PoS(LHCP2022)039

1. Introduction

By virtue of the factorisation theorem [1], the differential QCD cross section for $2 \rightarrow 2$ processes in hadron-hadron collisions can be written as a convolution of the partonic cross section $\hat{\sigma}(\vec{x}, \mu_R^2)$, which is of perturbative nature and depends on the renormalisation scale μ_R, with functions parameterising the non-perturbative properties of the initial and final states, *i.e.*

$$d\sigma = \sum_{i,j,a,b} \int_{\Omega} d^2\vec{x} d^2\vec{z}\ f_i(x_1, \mu_F^2) f_j(x_2, \mu_F^2) \times d\hat{\sigma}_{ij\rightarrow ab}(\vec{x}, \mu_R^2) \times D_a^h(z_3, \mu_f^2) D_b^h(z_4, \mu_f^2). \quad (1)$$

The initial state is characterised by the functions $f_i(x_j, \mu_F^2)$, which parameterise the fraction of momentum x carried by partons i and j, as a function of the factorisation scale μ_F. On the other hand, the final state is characterised by the fragmentation functions, $D_a^h(z, \mu_f^2)$, parameterising the fraction of momentum z carried by a hadron h when fragmented out of a final-state parton a as a function of the fragmentation scale μ_f.

The ATLAS and CMS detectors provide a unique environment for testing each of the components of Equation 1. This is achieved through the interpretation of different measurements, sensitive to each of the aspects mentioned above, by means of the comparison of the experimental data to different models.

2. The initial state: parton distribution functions

Determinations of the parton distribution functions have been published by both the ATLAS and CMS Collaborations [2, 3].

The ATLAS determination [2] makes use of a combination of deep inelastic scattering data from HERA [4], together with various ATLAS measurements at different values of the centre-of-mass energy: $\sqrt{s} = 7$, 8 and 13 TeV. This includes the production of W and Z bosons as well as photons, both inclusively and in association with jets. Measurements of inclusive jets and $t\bar{t}$ production are also considered. The measurements are compared to NNLO QCD + NLO EW predictions, which are then fitted to the data. The fit consists in the minimisation of a χ^2 function in a 21-dimensional parameter space, which fully takes into account the correlations between the measurements and their uncertainties. The results of the fit are compared to global PDF sets such as CT18 [5], NNPDF 3.1 [6] and MSHT20 [7].

The CMS determination [3] uses a combination of deep inelastic scattering data from HERA [4], together with triple-differential measurements of the $t\bar{t}$ cross section [8] and the double-differential inclusive jet cross section as a function of the jet transverse momentum and rapidity. The results are compared to approximate NNLO predictions for the inclusive jet cross section and NLO predictions for the triple-differential $t\bar{t}$ cross sections. Results for the top quark mass and the strong coupling constant are obtained together with the parton distribution functions.

Figure 1 shows the parton distribution function for the valence u-quark, determined from both the ATLAS and CMS analyses.

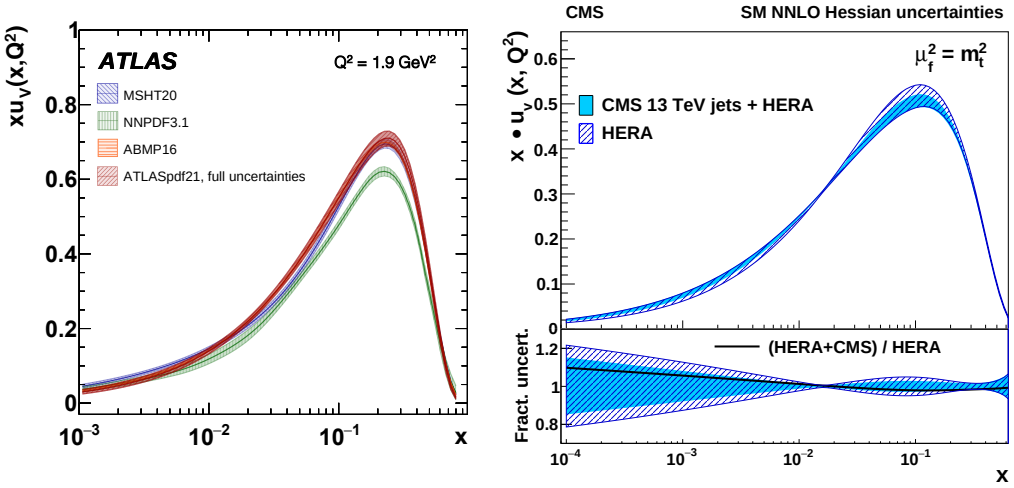

Figure 1: The valence u-quark parton density, $x \cdot u_v(x, Q^2)$ as determined from the ATLAS analysis at $Q^2 = 1.9$ GeV^2 (left, [2]) and the CMS analysis at $Q^2 = m_t^2$ (right, [3]).

3. The hard scattering: fixed-order matrix elements

Both ATLAS and CMS have recently published different measurements [3, 9–13] sensitive to the calculation of the fixed-order matrix element in Eq. 1. The data are compared to theoretical predictions at different orders of the perturbative expansion, up to NNLO pQCD.

- The inclusive jet cross section has been measured by CMS at different centre-of-mass energies of $\sqrt{s} = 5$ TeV [9] and $\sqrt{s} = 13$ TeV [3]. The results are compared to NLO and NNLO perturbative QCD predictions, including non-perturbative and electroweak corrections. The results show a very good agreement, within uncertainties, between the data and the NNLO predictions, while the NLO predictions tend to underestimate the data, in particular at central rapidities. As expected, the theoretical scale uncertainties on the NNLO predictions are significantly reduced with respect to NLO. Figure 2 shows the comparison of the measurements at $\sqrt{s} = 13$ TeV with the NNLO theoretical predictions.

- The Z+jets cross section has been measured in different contexts by both ATLAS and CMS. Reference [10] presents a measurement sensitive to double-parton scattering (DPS) from the azimuthal separation, as well as the momentum balance, between the Z boson and the leading jet or dijet system. The results for these distributions are compared to Monte Carlo predictions with different tunes. The simulation of multiple parton interactions is explicitly switched off for some of them, and the difference with respect to the data is evaluated. The left part of Figure 3 shows the $\Delta\phi$ distribution between the Z boson and the leading jet in inclusive Z+jets events, where the effect of DPS is clearly observed, see MPIOFF on the left plot of Fig. 3.

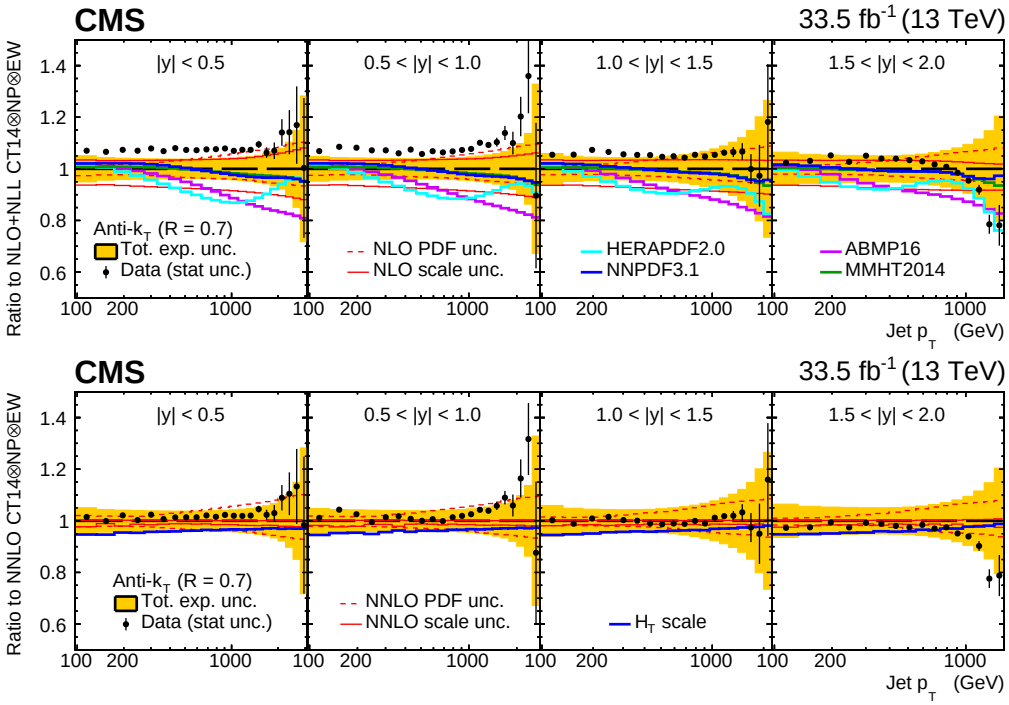

Figure 2: Ratio of the measured inclusive jet cross section with the NLO (top) and NNLO theoretical predictions (bottom) [9].

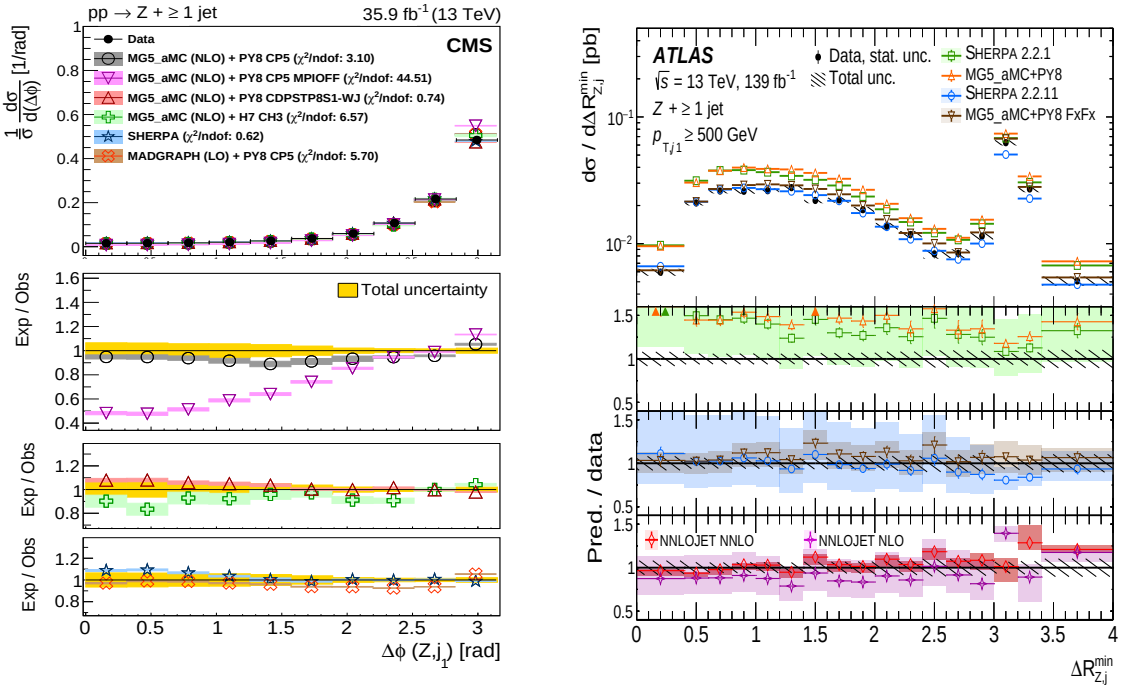

Figure 3: $\Delta\phi$ distribution between the Z boson and the leading jet in inclusive Z+jets events, showing the effect of double parton scattering (left, [10]). ΔR distribution between the Z boson and the closest high-pT jet in inclusive Z+jets events (right, [11]).

Reference [11] presents a measurement of the Z+jets cross section with high-p_T jets, as well as for different angular configurations between the Z boson and the leading jet. The results are compared to different theoretical predictions, including NNLO QCD predictions including electroweak corrections up to NLO. The results include a comparison of the ratio of the p_T of the Z boson to the p_T of the closest jet in collinear and back-to-back topologies. Reference [12] presents a measurement of the collinear versus large angle emissions, as well as soft versus hard radiation in Z+two-jet and three-jet final states. The measurements include the ratio p_{T3}/p_{T2}, as well as the angular distance ΔR_{23} between the second and the third hardest objects (including jets and Z bosons) in the events.

- The diphoton cross section is presented by ATLAS in Ref. [13]. Measurements are shown as a function of different kinematic variables including, among others, the invariant mass and the transverse momentum of the diphoton system, as well as the angular separation between the two photons. The results are compared to theoretical predictions up to NNLO.

4. The final state: heavy quark fragmentation functions

The fragmentation of heavy quarks into hadrons is explored by the ATLAS Collaboration in Refs. [14, 15]. Reference [14] presents a measurement of the fragmentation properties of charged B mesons, decaying through $B^{\pm} \to J/\psi K^{\pm}$, inside jets.

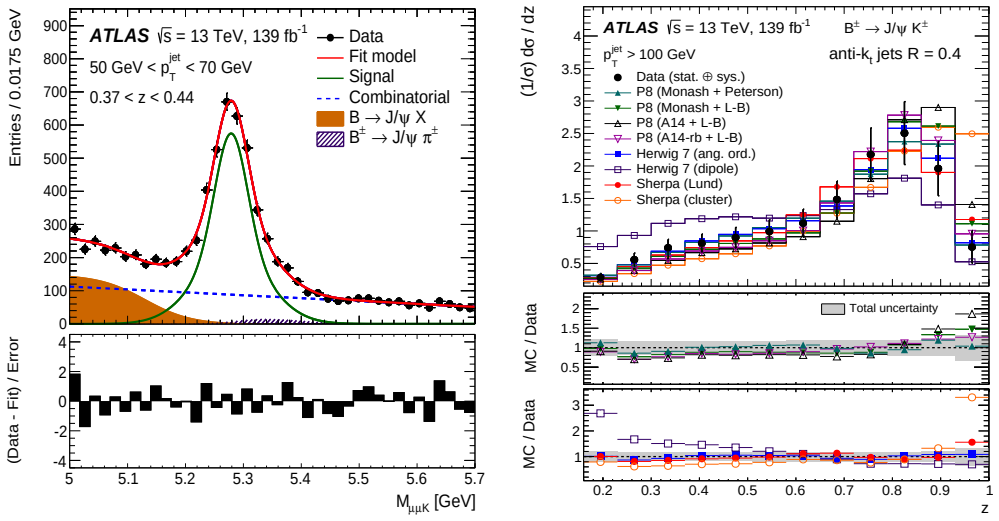

Figure 4: The invariant mass of the $B^{\pm}$ candidates reconstructed in a particular bin of jet p_T and z (left). The longitudinal profile distribution for jets with $p_T > 100$ GeV (right) [14]

More specifically, the longitudinal and transverse profiles of the momentum of $B^{\pm}$ mesons, $\vec{p}_B$, with respect to the momentum of the jets containing them, $\vec{p}_J$, defined as

$$z = \frac{\vec{p}_J \cdot \vec{p}_B}{|\vec{p}_J|^2}; \qquad p_T^{\text{rel}} = \frac{|\vec{p}_J \times \vec{p}_B|}{|\vec{p}_J|}, \tag{2}$$

are measured. The results show a significant dependence of the studied variables on the modelling of gluon splittings $g \to b\bar{b}$, and an important spread of the different Monte Carlo predictions with

respect to the data. Figure 4 shows the invariant mass of the reconstructed $B^{\pm}$ candidates, as well as the longitudinal profile for jets with $p_T > 100$ GeV.

Reference [15] presents a measurement of observables sensitive to the fragmentation functions of b-quarks in dileptonic $t\bar{t}$ events containing an electron and a muon. The measurement is performed using jets containing a displaced secondary vertex with at least four tracks originating from it, which are used to reconstruct the charged momentum of the B-hadron, $\vec{p}_b^{\,\mathrm{ch}}$. The charged momentum of the jet, $\vec{p}_{\mathrm{jet}}^{\,\mathrm{ch}}$, is reconstructed using all tracks geometrically associated to it.
The measured distributions, including the charged longitudinal profile as well as the number of charged tracks originating from the B-hadron decay, among others, are compared to different Monte Carlo expectations with the $t\bar{t}$ matrix elements calculated up to NLO, providing a generally reasonable agreement with the data.

5. Summary and conclusions

Results by the ATLAS and CMS Collaborations, sensitive to various aspects of the modelling of QCD, have been presented. The measurements include variables sensitive to the initial state, which are used for determining the Parton Distribution Functions, as well as to the hard-scattering process. The fragmentation of heavy quarks has been probed by ATLAS in two different analyses.

References

[1] J.C. Collins, D.E. Soper and G. Sterman, [Nucl. Phys. B. 261, 104 (1985)].

[2] ATLAS Collaboration, [Eur. Phys. J. C 82, 438 (2022)].

[3] CMS Collaboration, [JHEP 02, 142 (2022)].

[4] H1 and ZEUS Collaborations, [Eur. Phys. J. C 75, 580 (2015)].

[5] T-J. Hou *et al.*, [Phys. Rev. D 103, 014013 (2021)].

[6] R.D. Ball *et al.*, [Eur. Phys. J. C 77, 663 (2017)].

[7] S. Bailey *et al.*, [Eur. Phys. J. C 81, 341 (2021)].

[8] CMS Collaboration, [Eur. Phys. J. C 80, 658 (2020)].

[9] CMS Collaboration, [CMS-PAS-SMP-21-009].

[10] CMS Collaboration, [JHEP 10, 176 (2021)].

[11] ATLAS Collaboration, [arXiv:2205.02597 (hep-ex)].

[12] CMS Collaboration, [Eur. Phys. J. C 81, 852 (2021)].

[13] ATLAS Collaboration, [JHEP 11, 169 (2021)].

[14] ATLAS Collaboration [JHEP 12, 131 (2021)].

[15] ATLAS Collaboration [Phys. Rev. D 106, 032008 (2022)].